

# First Example of Low-Valence Ion Substitution in $\text{Ln}_5\text{O}(\text{OPr}^i)_{13}$ : Mixed-Valence Europium Oxoalkoxide $[\text{Eu}^{\text{III}}_4\text{Eu}^{\text{II}}\text{O}(\text{OPr}^i)_{12}(\text{HOPr}^i)]^*\text{HOPr}^i$

Marat Moustiakimov,<sup>†</sup> Mikael Kritikos,<sup>†</sup> and Gunnar Westin<sup>\*‡</sup>

Department of Structural Chemistry, Arrhenius Laboratory, Stockholm University, SE-106 91 Stockholm, Sweden, and Department of Materials Chemistry, Ångström Laboratory, Uppsala University, SE-751 21 Uppsala, Sweden

Received October 12, 2004

The novel mixed-valence alkoxide  $[\text{Eu}^{3+}_4\text{Eu}^{2+}\text{O}(\text{OPr}^i)_{12}(\text{HOPr}^i)]^*\text{HOPr}^i$  (**1**) has been prepared and structurally and spectroscopically characterized. The three synthesis routes (i) metathesis of  $4\text{EuCl}_3$ ,  $\text{EuI}_2$ , and  $14\text{KOPr}^i$  combined with hydrolysis with  $1\text{H}_2\text{O}$ , (ii) oxidation of  $5[\text{Eu}_4(\text{OPr}^i)_{10}(\text{HOPr}^i)_3]^*2\text{HOPr}^i$  with  $1.5\text{O}_2$ , and (iii) reduction of  $\text{Eu}_5\text{O}(\text{OPr}^i)_{13}$  with  $0.8[\text{Eu}_4(\text{OPr}^i)_{10}(\text{HOPr}^i)_3]^*2\text{HOPr}^i$  all yielded pure **1**, whereas (iv) reduction of  $\text{Eu}_5\text{O}(\text{OPr}^i)_{13}$  with 0.36–0.5 mol of europium metal produced impure **1**. The compound, having the average Eu oxidation number +2.8, is very sensitive toward further oxidation to  $\text{Eu}_5\text{O}(\text{OPr}^i)_{13}$  and is part of a redox series of europium 2-propoxides with average oxidation states +2.5, +2.8, and +3. The square pyramidal molecular structure, containing an oxo-oxygen atom in the basal plane, is similar to that of the well-known  $\text{Ln}_5\text{O}(\text{OPr}^i)_{13}$ ; the main difference is the substitution of an  $\text{Eu}^{3+}\text{-OPr}^i$  pair for an  $\text{Eu}^{2+}\text{-HOPr}^i$  pair in the basal plane. Fourier transform infrared (FT-IR) and UV–visible spectroscopy showed that the solid-state structure was retained on dissolution in hexane and toluene– $\text{HOPr}^i$ . The compound was further characterized by differential scanning calorimetry and solubility studies.

## 1. Introduction

In organic sol–gel processing, which has emerged as one of the key processes to obtain advanced ceramic thin films and nanostructured materials, alkoxides are the most important precursors.<sup>1</sup> The chemistry and structural features of the alkoxides are complicated and have proved elusive to predict, although much work has been done in this field during the past decade. But detailed knowledge of the alkoxide structure and chemistry is of great importance for a successful utilization of the full potential of these precursors. An area that has received considerable interest recently is the sol–gel processing of rare-earth doped glasses and ceramics as bulk, waveguide, and finely powdered materials.<sup>2</sup> In these

materials, lanthanide ion doping can be used for a number of applications, for example, signal enhancement and frequency upconversion in fibers and integrated optic devices and in different types of fluorescent displays. In the latter application Eu doping is of great importance.<sup>3</sup> Lanthanide alkoxides are also used in organic syntheses and for polymerization and are especially interesting since they do not leave poisonous residues.<sup>4</sup>

There have been some reports on the formation of europium alkoxides: Brown and Mazdiyasi<sup>5</sup> reported the formation of an alkoxide assumed to have the formula  $\text{Eu}(\text{OPr}^i)_2$  after refluxing the metal with a mercury-salt catalyst

\* To whom correspondence should be addressed. E-mail: Gunnar.Westin@mkem.uu.se.

<sup>†</sup> Stockholm University.

<sup>‡</sup> Uppsala University.

- (1) (a) Chandler, C. D.; Rogers, C.; Hampden-Smith, M. J. *Chem. Rev.* **1993**, *93*, 1205. (b) Brinker, C. J.; Scherer, G. W. *The Physics and Chemistry of Sol–Gel Processing*; Academic Press: London, 1990.
- (2) (a) Weber, M. J. *J. Non-Cryst Solids* **1990**, *123*, 208. (b) Westin, G.; Ekstrand, A.; Zanghellini, E.; Börjesson, L. *J. Phys. Chem. Solids* **2000**, *61*, 67. (c) Yeh, D. C.; Sibley, W. A.; Suscavage, M.; Drexhage, M. G. *J. Appl. Phys.* **1987**, *62*, 266. (d) Shinn, M. D.; Sobley, W. A.; Drexhage, M. G.; Brown, R. N. *Phys. Rev.* **1983**, *27*, 6635. (e) Desurvire, E. *Phys. Today* **1994**, *Jan*, 20.

- (3) (a) Nageno, Y.; Takebe, H.; Morinaga, K.; Izumitani, T. *J. Non-Cryst. Solids* **1994**, *169*, 288. (b) Piriou, B.; Chen, Y. F.; Vilminot, S. *Eur. J. Solid State Inorg. Chem.* **1998**, *35*, 341. (c) Pillonet-Minardi, A.; Marty, O.; Bovier, C.; Carapon, C.; Mugnier, J. *Opt. Mater.* **2001**, *16*, 9.
- (4) (a) Aspinall, H. C. *Chem. Rev.* **2002**, *102*, 1807. (b) Yasuda, H. *Prog. Polym. Sci.* **2000**, *25*, 573. (c) Evans, D. A.; Nelson, S. G.; Gagne, M. R.; Muci, A. R. *J. Am. Chem. Soc.* **1993**, *115*, 9800. (d) Bougauchi, M.; Watanabe, S.; Arai, T.; Sasai, H.; Shibasaki, M. *J. Am. Chem. Soc.* **1997**, *119*, 2329. (e) Chen, R. F.; Qian, C. T.; de Vries, J. G. *Tetrahedron* **2001**, *57*, 9837. (f) Chen, R. F.; Qian, C. T.; de Vries, J. G. *Tetrahedron Lett.* **2001**, *42*, 6919. (g) Gromada, J.; Mortreux, A.; Chenal, T.; Ziller, J. W.; Leising, F.; Carpentier, J.-F. *Chem.-Eur. J.* **2002**, *8*, 3773.
- (5) Brown, L. M.; Mazdiyasi, K. S. *Inorg. Chem.* **1970**, *9*, 2783.

in 2-propanol-containing solvents. Evans et al. reported that dissolution of the metal without a catalyst below 45 °C yielded a divalent europium 2-propoxide, which yielded a product formulated as  $\text{Eu}(\text{OPr}^i)_2(\text{THF})_x$ ,<sup>6</sup> after dissolution in tetrahydrofuran (THF). Dissolution of Eu in methoxyethanol yielded the corresponding methoxyethoxide formulated as  $\text{Eu}(\text{OC}_2\text{H}_4\text{OCH}_3)_2$ .<sup>7</sup> An unusual mixed-valence alkoxocarbitoxide complex,  $\text{Eu}_3[(\text{OCH}_2\text{CH}_2\text{O})_2\text{CH}_2\text{CH}_3]_4(\text{OC}_6\text{H}_5\text{Pr}^{2-2,6})_3$  has also been reported by the same group.<sup>8</sup> The only homometallic europium alkoxides, containing only oxo or hydroxo groups in addition to the alkoxo groups, that have been structurally determined by X-ray techniques are  $[\text{Eu}_4(\text{OPr}^i)_{10}(\text{HOPr}^i)_3] \cdot 2\text{HOPr}^i$  and  $\text{Eu}_5\text{O}(\text{OPr}^i)_{13}$ .<sup>9</sup> The former was obtained by dissolving europium metal in a 2-propanol-containing solvent at temperatures up to 65–70 °C, and the latter by metathesis of  $5\text{EuCl}_3$  and  $15\text{KOPr}^i$  hydrolyzed with  $1\text{H}_2\text{O}$ . The latter compound could also be obtained by oxidation with dioxygen of the mixed  $\text{Eu}^{2+}/\text{Eu}^{3+}$  alkoxide  $[\text{Eu}_4(\text{OPr}^i)_{10}(\text{HOPr}^i)_3] \cdot 2\text{HOPr}^i$ .<sup>9</sup> The structurally characterized heterometallic europium alkoxides are limited to  $\text{EuNa}_8(\text{OH})(\text{OBU}^t)_{10}$ ,<sup>10</sup>  $\text{EuSn}_2(\text{OBU}^t)_6$ ,<sup>11</sup> and  $\text{EuAl}_3(\text{OPr}^i)_{12}$ .<sup>9</sup> Other mixed-valence lanthanide alkoxides reported to date include  $\text{Ce}_4\text{O}(\text{OPr}^i)_{13}(\text{HOPr}^i)$ .<sup>12</sup> As in  $[\text{Eu}_4(\text{OPr}^i)_{10}(\text{HOPr}^i)_3] \cdot 2\text{HOPr}^i$ , it has a “butterfly” type arrangement of the metal atoms. In the Ce compound, three  $\text{Ce}^{4+}$  and one  $\text{Ce}^{3+}$  ions are delocalized within four positions, while in the Eu molecule two  $\text{Eu}^{2+}$  are situated at wingtip and two  $\text{Eu}^{3+}$  at hinge positions.

In the present study, we report the mixed  $\text{Eu}^{2+}/\text{Eu}^{3+}$  2-propoxide  $[[\text{Eu}_4\text{EuO}(\text{OPr}^i)_{12}(\text{HOPr}^i)]] \cdot \text{HOPr}^i$  (**1**), which is structurally and electrochemically closely related to the previously reported  $\text{Eu}_5\text{O}(\text{OPr}^i)_{13}$ .<sup>9</sup> This third Eu 2-propoxide has an average oxidation state of +2.8 and could, interestingly, be prepared both by oxidation of  $[\text{Eu}_4(\text{OPr}^i)_{10}(\text{HOPr}^i)_3] \cdot 2\text{HOPr}^i$  and by reduction of  $\text{Eu}_5\text{O}(\text{OPr}^i)_{13}$ . The square pyramidal structure with an oxo-oxygen in the basal plane is very similar to that of  $\text{Eu}_5\text{O}(\text{OPr}^i)_{13}$ , but here one of the basal  $\text{Eu}^{3+}$  ions is replaced by an  $\text{Eu}^{2+}$  ion with a 2-propanol group as adduct instead of an alkoxo group. This is the first example of an  $\text{Ln}_5\text{O}(\text{OPr}^i)_{13}$  molecule with a low-valent ion substitution and shows that it is possible to put in both higher and lower charged ions of quite different size compared to the  $\text{Ln}^{3+}$  ions and that they take predictable positions in the square pyramidal molecule. It has already been shown that, with metal ions having a higher electronegative character than the  $\text{Ln}^{3+}$  ions, substitution takes place at the apex position, such as in  $\text{Ln}_4\text{TiO}(\text{OPr}^i)_{14}$ <sup>13</sup> and  $\text{Er}_4\text{SbO}(\text{OPr}^i)_{13}$ ,<sup>14</sup> while with less electronegative ions such as  $\text{Eu}^{2+}$  and  $\text{Sr}^{2+}$ ,<sup>14</sup>

the substitution occur at the base-plane positions. This makes it possible to use the structurally very flexible homometallic  $\text{Ln}_5\text{O}(\text{OPr}^i)_{13}$  molecule, present for all Ln ions, as a base to obtain tailored heterometallic alkoxides. This knowledge provides a tool for the preparation of purpose-built heterometallic oxoalkoxides based on the  $\text{M}_5\text{O}$  structure. When the compound is considered in the context of a mixed-valence compound, it is of interest that the  $\text{Eu}^{2+}$  ion seem not to take part in redox chemistry with its neighboring  $\text{Eu}^{3+}$  ions, which is in contrast to what has been reported for the mixed-valence  $\text{Ce}_4\text{O}(\text{OPr}^i)_{13}(\text{HOPr}^i)$  molecule.<sup>12</sup> The structure of **1** was determined by single-crystal X-ray techniques and it was characterized by differential scanning calorimetry, IR and UV–vis spectroscopy, and solubility studies.

## 2. Experimental Section

**2.1. Equipment and Chemicals.** The elemental contents (Eu, K, Cl, and I) were obtained from air-hydrolyzed and gently dried samples, by use of a scanning electron microscope (SEM, JEOL 820) with an energy-dispersive X-ray spectrum analyzer (EDS, Link AN 10000). These elements can normally be detected down to ca. 0.3 at. %. Fourier transform infrared (FT-IR) spectra, in the range 5000–370  $\text{cm}^{-1}$ , were obtained with a Bruker IFS-55 spectrometer. The solid samples were investigated as paraffin mulls, and the dissolved samples, in a 0.1 mm path-length KBr cell. UV–Vis spectra, in the range 300–800 nm, were obtained at ambient temperature with a Perkin-Elmer Lambda 19 dispersive spectrometer with a <0.25 nm slit. The solutions were analyzed in sealed quartz cuvettes and the solid materials in transmittance mode, in quartz cuvettes in front of a 60 mm integrated reflectance sphere. Up to 80 scans were collected to obtain sufficiently good average signal-to-noise ratio. The behavior on heating in the range 25–250 °C, at a heating rate of 5 °C·min<sup>-1</sup>, was studied with a differential scanning calorimeter (DSC, Perkin-Elmer DSC-2) with airtight steel compartments. Crystals in sealed glass capillaries were studied during heating at temperatures up to 300 °C in a solid-block melting-point apparatus.

The syntheses and recrystallizations, the sample preparations for DSC, IR, and UV–vis spectroscopic studies and for visual observation during heating, and the mounting of crystals for single-crystal X-ray data collection were performed in a glovebox containing dry, oxygen-free argon. The glassware was dried at 150 °C for more than 30 min before being taken into the glovebox. The toluene, tetrahydrofuran (THF), and 2-propanol ( $\text{HOPr}^i$ ) were dried by distillation over  $\text{CaH}_2$ . The  $\text{C}_2\text{H}_4\text{I}_2$  (1,2-diiodoethane, Aldrich) was used as purchased. The oxygen gas used in the oxidation experiments was dried with  $\text{P}_2\text{O}_5$ . The Eu metal (99.9%, Strem Chemicals) and anhydrous  $\text{EuCl}_3$  (99.9%, Strem Chemicals) were used as purchased.  $[\text{Eu}_4(\text{OPr}^i)_{10}(\text{HOPr}^i)_3] \cdot 2\text{HOPr}^i$  and  $\text{Eu}_5\text{O}(\text{OPr}^i)_{13}$  were prepared according to the literature by metal dissolution in  $\text{HOPr}^i$ -containing solvent and by metathesis–hydrolysis with  $\text{EuCl}_3$  and  $\text{KOPr}^i$ , respectively.<sup>9</sup>

**2.2. Synthesis of  $[\text{Eu}_4\text{EuO}(\text{OPr}^i)_{12}(\text{HOPr}^i)] \cdot \text{HOPr}^i$  (**1**). Metathesis–Hydrolysis.** An  $\text{Eu}_2 \cdot \text{THF}_x$  complex was prepared from europium metal and  $\text{C}_2\text{H}_4\text{I}_2$  in THF solvent according to the procedure described by Girard et al.<sup>15</sup> for Yb and Sm, followed by removal

(6) Evans, W. J.; Greci, M. A.; Ziller, J. W. *Inorg. Chem.* **2000**, *39*, 3213.

(7) Evans, W. J.; Greci, M. A.; Ziller, J. W. *Inorg. Chem.* **1998**, *37*, 5221.

(8) Evans, W. J.; Greci, M. A.; Ziller, J. W. *Inorg. Chem. Commun.* **1999**, *2*, 530.

(9) Westin, G.; Moustiakimov, M.; Kritikos, M. *Inorg. Chem.* **2002**, *41*, 3249.

(10) Evans, W. J.; Sollenberger, M. S.; Ziller, J. W. *J. Am. Chem. Soc.* **1993**, *115*, 4120.

(11) (a) Veith, M.; Hans, J.; Stahl, L.; May, P.; Huch, V.; Sebald, A. Z. *Naturforsch., B: Chem. Sci.* **1991**, *46*, 403. (b) *Chem. Ber.* **1992**, *125*, 1033.

(12) Yunlu, K.; Gradeff, P. S.; Edelstein, N.; Kot, W.; Shalimoff, G.; Streib, W. E.; Vaarstra, B. A.; Caulton, K. G. *Inorg. Chem.* **1991**, *30*, 2317.

(13) (a) Daniele, S.; Hubert-Pfalzgraf, L. G.; Daran, J. C.; Halut, S. *Polyhedron* **1994**, *13*, 2163. (b) Moustiakimov, M.; Kritikos, M.; Westin, G. (Tb,Er)<sub>4</sub>TiO(OiPr)<sub>14</sub>, *Acta Crystallogr.* **1998**, *C54*, 29.

(14) Unpublished results.

of the THF groups by heating in a vacuum (ca.  $5 \times 10^{-2}$  Torr) at 140 °C for 4 h. The resulting pale green powder yielded an IR spectrum containing only extremely weak peaks due to organic groups. Typically, 5.54 mmol (0.217 g) of potassium was dissolved in 20 mL of 1:1 (v/v) toluene/HOPr<sup>i</sup>, and 0.39 mL of 1 M H<sub>2</sub>O in toluene/HOPr<sup>i</sup> was added. Then, 1.58 mmol (0.409 g) of EuCl<sub>3</sub> and 3.97 mmol (0.161 g) of EuI<sub>2</sub> were added, and after 48 h at room temperature, the mixture was centrifuged to separate the pale yellow sediment. This precipitate was analyzed by SEM-EDS and found to contain K, Cl, and I and ca. 5% Eu. On evaporation of the yellow solution part, a dark yellow mass of **1** was obtained in a yield of ca. 75%. The yield was increased by washing the salt precipitate three times with toluene/2-propanol to yield a salt mixture virtually free of Eu, according to the SEM-EDS studies. SEM-EDS analyses showed no signals from K, Cl, or I in the alkoxides obtained from the solvent phase.

**Oxidation of  $[\text{Eu}_4(\text{OPr}^i)_{10}(\text{HOPr}^i)_3] \cdot 2\text{HOPr}^i$ .**  $[\text{Eu}_4(\text{OPr}^i)_{10}(\text{HOPr}^i)_3] \cdot 2\text{HOPr}^i$  (0.148 mmol, 0.222 g) was dissolved in 5 mL of (2:3) toluene/HOPr<sup>i</sup>. Then, 0.0445 mmol (based on a molar volume of 24.0 mol dm<sup>-3</sup>) (1.07 mL) of dioxygen was added with a gastight syringe under stirring. A very slight reduction in the strength of the yellow color was observed during the first 10 min. Evaporation of the solution in a vacuum after 3 h yielded a dark yellow mass whose IR spectrum was consistent with that of well-shaped crystals of **1**. Yield ca. 100%.

**Reduction of  $\text{Eu}_5\text{O}(\text{OPr}^i)_{13}$  with Eu Metal.** Europium metal was added to 0.2 M toluene/HOPr<sup>i</sup> (2:1) solutions of  $\text{Eu}_5\text{O}(\text{OPr}^i)_{13}$ , with Eu: $\text{Eu}_5\text{O}(\text{OPr}^i)_{13}$  ratios of 0.36, 0.40, 0.50, 1.0, and 2.0. A strong yellow coloration appeared within minutes, and after 1 h a small amount of a fine brownish-red powder had been formed. After 4 h at room temperature, the yellow solution was separated from the powder (which had formed to an extent of ca. 5% of the metal added) and slowly evaporated under vacuum to form a dark yellow mass. The products were identified by IR spectroscopy to be mainly **1**, with the 1:0.36–1:0.50 ratios producing the purest product.

**Reduction of  $\text{Eu}_5\text{O}(\text{OPr}^i)_{13}$  with  $[\text{Eu}_4(\text{OPr}^i)_{10}(\text{HOPr}^i)_3] \cdot 2\text{HOPr}^i$ .**  $\text{Eu}_5\text{O}(\text{OPr}^i)_{13}$  (0.144 mmol, 0.222 g) and  $[\text{Eu}_4(\text{OPr}^i)_{10}(\text{HOPr}^i)_3] \cdot 2\text{HOPr}^i$  (0.120 mmol, 0.180 g) were mixed in 10 mL of toluene/HOPr<sup>i</sup> (1:1). Four hours later, the mixture was evaporated almost to dryness in a vacuum. The obtained yellow mass of liquid and crystals was identified by IR spectroscopy as pure **1**, yield ca. 100%. When a stoichiometric amount of water, 0.095 mmol (0.095 mL of 1 M H<sub>2</sub>O in toluene/HOPr<sup>i</sup>), was slowly added after the mixing of the alkoxides, the solution became slightly turbid and a minor amount of insoluble material formed, which somewhat reduced the yield of the main product, **1**.

**2.3. Data for Identification.** IR and UV–vis spectra of well-formed crystals of **1** are shown in Figures 1 and 2, respectively. Mp (DSC): 72–74 °C, (vide infra). Selected peaks for identification: IR (paraffin mull), 1174sh, 1164, 1126, 1000, 975, 959, 835, 824, 523, 484, 445, 433sh, 408, 396sh, 387sh, 384, and 379 cm<sup>-1</sup>, and UV–vis (toluene/HOPr<sup>i</sup> 4:1), 524.3, 530.6, 532.6sh, and 576.3 nm. Compound **1** is very soluble in toluene and hexane but only slightly soluble in HOPr<sup>i</sup>. Elongated rhombic crystals formed about 1–2 days after addition of toluene/HOPr<sup>i</sup> to dissolve almost all of the alkoxide powder first obtained. Compound **1** is rather stable in the form of well-shaped crystals in a strictly oxygen- and moisture-free atmosphere, although it decomposes over periods of many months.

**2.4. Structure Determinations.** A large crystal of **1** was cut into smaller crystallites that were glued with a very small amount

**Table 1.** Crystallographic Data for **1**

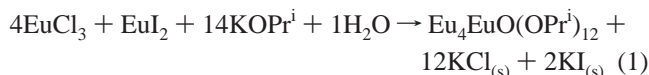
empirical formula	C <sub>42</sub> H <sub>100</sub> Eu <sub>5</sub> O <sub>15</sub>
fw	1605.02
crystal system, space group	triclinic, <i>P1</i>
<i>a</i> (Å)	12.981(2)
<i>b</i> (Å)	13.134(2)
<i>c</i> (Å)	21.336(3)
$\alpha$ (deg)	98.21(2)
$\beta$ (deg)	98.86(2)
$\gamma$ (deg)	118.13(1)
<i>V</i> (Å <sup>3</sup> )	3071.3(6)
<i>Z</i>	2
<i>T</i> (K)	110(2)
$\rho_{\text{calc}}$ (g/cm <sup>3</sup> )	1.736
$\mu$ (Mo K $\alpha$ ) (mm <sup>-1</sup> )	5.081
absolute structure parameter	0.05(3)
data/restraints/parameters	19 412/74/1017
goodness-of-fit on $F^2$	1.032
$R1^a$ ( $F_o$ ), $wR2^a$ ( $F_o^2$ )	0.0734, 0.1873

$$^a R1 = \sum ||F_o| - |F_c|| / \sum |F_o|; wR2 = [\sum [w(F_o^2 - F_c^2)^2] / \sum [w(F_o^2)^2]]^{1/2}.$$

of paraffin in glass capillaries, which were subsequently melt-sealed. Single-crystal X-ray diffraction data from a chosen crystal were collected on a Stoe image-plate diffractometer at 110 K. Selected crystallographic and experimental data together with the refinement details are given in Table 1. There were no systematic absences in the collected diffraction data; the space group assigned was *P1* (No. 1). The data were corrected for absorption effects by use of the X-SHAPE program package.<sup>16</sup> The structure was solved by direct methods and refined against  $F^2$  by use of the computer programs SHELXS97<sup>17</sup> and SHELXL97,<sup>18</sup> respectively. A number of 2-propyl groups were refined as disordered. Hydrogen atoms were added at ideal positions and refined by use of a riding model with thermal displacement parameters 1.2 times the  $U_{\text{iso}}$  of their respective pivot atoms. Further details on the refinement are provided as Supporting Information.

### 3. Results and Discussion

**3.1. Synthesis.** The best controllable and most straightforward route to **1** is metathesis with europium halides having the right total oxidation number of the Eu ions, in combination with stoichiometric hydrolysis to yield the oxo-oxygen according to reaction 1. This route produces high yields of **1** and yields no byproducts difficult to remove.



In the search for a proper expression for oxidation of  $[\text{Eu}_4(\text{OPr}^i)_{10}(\text{HOPr}^i)_3] \cdot 2\text{HOPr}^i$  by dioxygen, no straightforward equation could be conceived. Enough oxo-oxygens could not be obtained in eq 2, so that a fourth of the europium atoms would end up in non-oxoalkoxides. With the highly basic character of the product non-oxoalkoxides, however, these alkoxides should be rather labile and tend to decompose to the oxoalkoxide **1**, in accordance with the findings for other

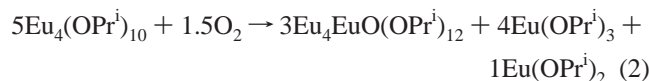
(16) *Crystal Optimisation for Numerical Absorption Correction*, X-SHAPE revision 1.09; Stoe: Darmstadt, Germany, 1997.

(17) Sheldrick, G. M. *Acta Crystallogr.* **1994**, *A46*, 467.

(18) Sheldrick, G. M. *SHELX97. Computer Program for the Refinement of Crystal Structures*, Release 97-2 ed.; Sheldrick, G. M., Ed.; University of Göttingen: Göttingen, Germany, 1997.

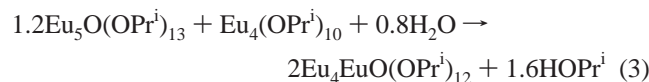
(15) Girard, P.; Namy, J. L.; Kagan, H. B. *J. Am. Chem. Soc.* **1980**, *102*, 2693.

non-oxo-2-propoxides of lanthanides.<sup>19–21</sup> Little is known about the decomposition pathways of alkoxides, but ether, acetone, propene, and propane have been found as products in other studies.<sup>22,23</sup> The observed complete conversion of  $[\text{Eu}_4(\text{OPr}^i)_{10}(\text{HOPr}^i)_3] \cdot 2\text{HOPr}^i$  into **1** indicates that non-oxoalkoxides, if formed, ought to autodecompose, although no ethers or other organic decomposition products were observed.



Thus, the oxidation of  $[\text{Eu}_4(\text{OPr}^i)_{10}(\text{HOPr}^i)_3] \cdot 2\text{HOPr}^i$  is also efficient and does not yield any byproducts but requires a well-defined  $[\text{Eu}_4(\text{OPr}^i)_{10}(\text{HOPr}^i)_3] \cdot 2\text{HOPr}^i$  material, free from residual solvent, to deliver the proper stoichiometry. This is best achieved by dissolving europium metal to form  $[\text{Eu}_4(\text{OPr}^i)_{10}(\text{HOPr}^i)_3] \cdot 2\text{HOPr}^i$  and adding oxygen without intermediate workup.

Reduction of  $\text{Eu}_5\text{O}(\text{OPr}^i)_{13}$  with  $[\text{Eu}_4(\text{OPr}^i)_{10}(\text{HOPr}^i)_3] \cdot 2\text{HOPr}^i$  according to eq 3 was attempted:



The reaction proceeded to **1** but with the formation of a small amount of solid powder, believed to be a hydrolysis product. Without addition of water, however, the sole product was **1**. Thus, it seems that decomposition to the oxoalkoxide occurs rapidly after mixing of the alkoxides, and the water added according to reaction 3 will then hydrolyze some of the **1** already formed.

No obvious equation could be formulated for reduction of  $\text{Eu}_5\text{O}(\text{OPr}^i)_{13}$  with Eu metal, but the most probable ones were obtained in the range  $\text{Eu}:\text{Eu}_5\text{O}(\text{OPr}^i)_{13} = 0.36\text{--}0.43$ . The experimental observations indicated that **1** formed in maximum yield in the range  $\text{Eu}:\text{Eu}_5\text{O}(\text{OPr}^i)_{13} = 0.36\text{--}0.50$ , but the IR spectra showed that it was never completely pure, and a small amount of insoluble brownish-red powder was observed to form during the reaction. Unfortunately, the attempts to obtain X-ray diffraction (XRD) patterns of samples between double gastight polyimide (Kapton) tapes of the powder were unsuccessful, due to decomposition of the sample shown by gas formation and a lightening of the sample. The XRD pattern of the resulting powder could not be interpreted with any certainty. The IR spectrum showed no peaks associated with organic groups, hydroxyl or carbonate groups. The strong peaks were very broad;  $400\text{--}800\text{ cm}^{-1}$  with maximum at  $620\text{ cm}^{-1}$  and a shoulder at ca.  $720\text{ cm}^{-1}$ , and  $900\text{--}1100\text{ cm}^{-1}$  with a maximum at  $960\text{ cm}^{-1}$

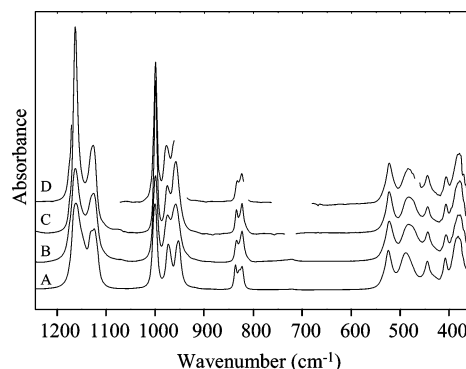
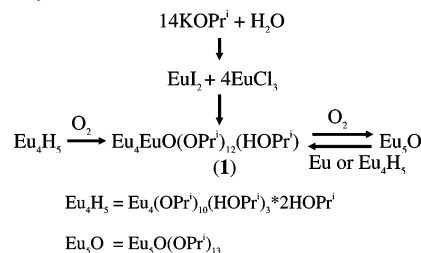


**Figure 1.** IR spectra of  $\text{Eu}_5\text{O}(\text{OPr}^i)_{13}$  as solid in paraffin mull (A), **1** as solid in paraffin mull (B), **1** in hexane solution (C), and **1** in toluene/ $\text{HOPr}^i$  (1:2) solution (D). The graph has been removed where proper background-subtraction of solvent peaks could not be made due to a very strong signal.

#### Scheme 1. Synthesis and Reaction Overview



and a shoulder at ca.  $1030\text{ cm}^{-1}$ , while the weak peaks were narrow and found in groups of 5–7 around  $830$  and  $1150\text{ cm}^{-1}$ . The IR data and color fit rather well to the data reported for  $\text{EuH}_{1.85}$  prepared from the elements,<sup>24</sup> and the color is typical of europium hydrides, which indicates that the brownish-red product is  $\text{EuH}_{2-x}$ . The hydride formation in this reaction, but not when the metal is dissolved in  $\text{HOPr}^i$ /toluene, is difficult to understand.

It is also possible that the dissolved europium metal reacts to some extent to form  $[\text{Eu}_4(\text{OPr}^i)_{10}(\text{HOPr}^i)_3] \cdot 2\text{HOPr}^i$ , having an average Eu oxidation number of +2.5, thereby diminishing the expected reductive power of the europium metal during the reduction of  $\text{Eu}_5\text{O}(\text{OPr}^i)_{13}$ . Therefore this seems to be a less versatile route.

Thus, **1** can be reached from alkoxides with both higher and lower average oxidation states, and so, this compound is part of an oxidation-state series:  $[\text{Eu}_4(\text{OPr}^i)_{10}(\text{HOPr}^i)_3] \cdot 2\text{HOPr}^i$  (+2.5),  $\text{Eu}_5\text{O}(\text{OPr}^i)_{12}(\text{HOPr}^i)$  (+2.8) (**1**), and  $\text{Eu}_5\text{O}(\text{OPr}^i)_{13}$  (+3) (Scheme 1). From these studies, it seems that it is not possible to remove an  $\text{O}^{2-}$  ion once introduced to the alkoxide, even in the presence of very strong oxophiles such as  $\text{Eu}^{2+}$ .

**3.2. Properties: IR Spectroscopy.** IR spectra of **1** are shown in Figure 1. The peak maxima in the fingerprint region  $1200\text{--}370\text{ cm}^{-1}$  are assigned as follows:  $1200\text{--}800\text{ cm}^{-1}$ , C–O and C–C stretching and bending and  $550\text{--}370\text{ cm}^{-1}$ , Eu–O stretching. A hydroxyl stretch band with a maximum at  $3188\text{ cm}^{-1}$  and a shoulder at ca.  $3330\text{ cm}^{-1}$ , tailing down to ca.  $2900\text{ cm}^{-1}$ , indicates hydrogen bonds of medium strength. The IR spectra of solid and dissolved **1** are quite

(19) Poncetlet, O.; Sartain, W. J.; Hubert-Pfalzgraf, L. G.; Foltling, K.; Caulton, K. G. *Inorg. Chem.* **1989**, *28*, 263.

(20) Helgesson, G.; Jagner, S.; Poncetlet, O.; Hubert-Pfalzgraf, L. G. *Polyhedron* **1991**, *10*, 1559.

(21) Westin, G.; Kritikos, M.; Wijk, M. *J. Solid State Chem.* **1998**, *141*, 168.

(22) Vaartstra, B. A.; Streib, W. E.; Caulton, K. G. *J. Am. Chem. Soc.* **1990**, *112*, 8593.

(23) Turova, N. Ya.; Kessler, V. G.; Kucheiko, S. I. *Polyhedron* **1991**, *10*, 2617.

(24) (a) Drulis, M. *J. Alloys Compd.* **1993**, *198*, 111. (b) Willson, S. P.; Andrews, L. *J. Phys. Chem. A* **2000**, *104*, 1640.

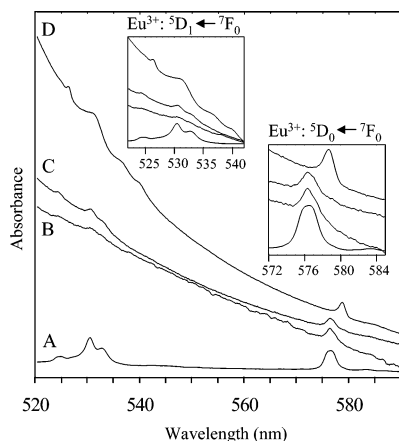


**Figure 2.** Electronic spectra of  $\text{Eu}_5\text{O}(\text{OPr}^i)_{13}$  solution (A), solid **1** (B), toluene/ $\text{HOPr}^i$  (4:1) solution of **1** (C), and  $[\text{Eu}_4(\text{OPr}^i)_{10}(\text{HOPr}^i)_3] \cdot 2\text{HOPr}^i$  solution (D).

similar, indicating that the solid-state molecular entities are nearly unchanged in solution. In hexane solution, the OH stretch maximum was found at  $3202\text{ cm}^{-1}$  together with a shoulder at ca.  $3330\text{ cm}^{-1}$ , very close to the values found for the solid material, which indicates that the hydrogen bonds are almost unaffected by dissolution in a nonpolar solvent. As can be seen in Figure 1, the spectrum of **1** is very similar to that of  $\text{Eu}_5\text{O}(\text{OPr}^i)_{13}$ , especially in the Eu–O stretch area. The compounds can most easily be distinguished by comparing the C–O and C–C vibrations.

**UV–Vis Spectroscopy.** The electronic transition spectra of solid and dissolved **1** are shown in Figure 2. The spectra show a strong band, assigned as due to the  $\text{Eu}^{2+}$  ions, extending from the UV region to ca. 550–600 nm and causing the strong orange-yellow color of the compound. In earlier work, we have shown that the fine structure of the absorptions in the UV–vis–NIR region can be used to study even very subtle changes in the coordination geometry of  $\text{Ln}^{3+}$  ions, making it possible to distinguish between differently coordinated  $\text{Ln}^{3+}$  ions even with the same coordination number and only oxygen donor ligands.<sup>9,21,25,26</sup>  $\text{Eu}^{3+}$  is also suitable for such studies, and the assignments have been made after the scheme reported by Yatsimirskii and Davidenko.<sup>27</sup> The very weak peaks, assigned as due to the  $^5\text{D}_1 \leftarrow ^7\text{F}_0$  [524.3, 530.6, and 532.6(sh) nm] and  $^5\text{D}_0 \leftarrow ^7\text{F}_0$  (576.3 nm) transitions within the  $\text{Eu}^{3+}$  ions, were very similar in shape and position in the solid and dissolved states, which thus corroborates the indication of retained molecular structure in the solution found by the IR spectroscopy studies. The positions and shapes of the peaks due to the  $\text{Eu}^{3+}$  ions are similar to those of  $\text{Eu}_5\text{O}(\text{OPr}^i)_{13}$ , but quite different from those in the non-oxoalkoxide  $[\text{Eu}_4(\text{OPr}^i)_{10}(\text{HOPr}^i)_3] \cdot 2\text{HOPr}^i$ , as can be seen in Figure 2. This seems natural in light of the very similar coordination figures of the  $\text{Eu}^{3+}$  ions in the two square pyramidal oxoalkoxides and the different coordination

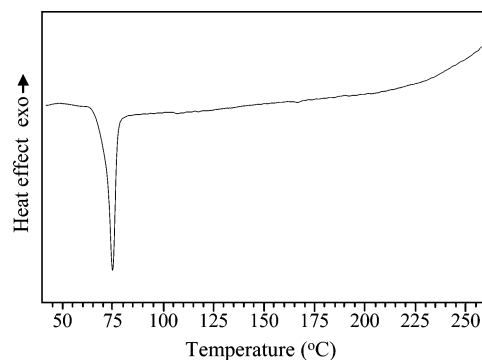


**Figure 3.** DSC graph of **1** obtained under inert atmosphere at  $5\text{ °C}\cdot\text{min}^{-1}$ .

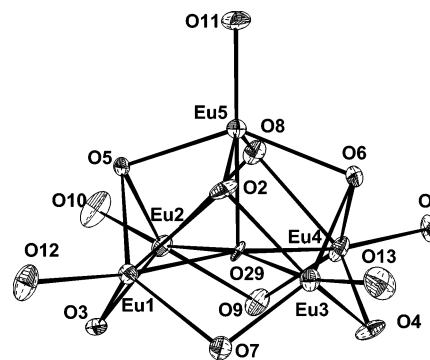


**Figure 4.** ORTEP view (30% probability displacement ellipsoids) showing the molecular structure of the metal–oxygen core of the two different molecules in **1**.

in the non-oxoalkoxide, although all  $\text{Eu}^{3+}$  ions are octahedrally coordinated by oxygen donor ligands.

**Behavior on Heating.** Crystals in sealed glass capillaries began to appear moist and sintered to some degree in the temperature range 55–75 °C and melted to a clear brown liquid around 200–230 °C. Loss of liquid with condensation in the cold end of the capillary was observed from 190 °C, and a clear yellow residue remained after heating to 300 °C. In the DSC graph, shown in Figure 3, an endothermic peak corresponding to ca.  $20\text{ kJ}\cdot\text{mol}^{-1}$  starts at ca. 60 °C, with an onset at 72 °C and a minimum at 75 °C that corresponds to the observed first densification. This energy is close to those observed for the sintering without visible melting for other compounds in the  $\text{Ln}_5\text{O}(\text{OPr}^i)_{13}$  series, which are in the range 5–20  $\text{kJ}\cdot\text{mol}^{-1}$ , but it is lower than expected for a complete loss of solvating  $\text{HOPr}^i$  groups.<sup>9,21,25,28</sup>

**3.3. Structure.** The molecular structure of **1** is shown in Figure 4. Selected bond lengths and angles for **1** are given in Table 2. The asymmetric unit of this alkoxide consists of two independent  $[\text{Eu}_5\text{O}(\text{OPr}^i)_{12}(\text{HOPr}^i)] \cdot [\text{HOPr}^i]$  bimolecular units. The  $[\text{Eu}_5\text{O}(\text{OPr}^i)_{12}(\text{HOPr}^i)]$  molecule contains five Eu atoms, one oxo oxygen, and 13 2-propoxo groups, namely, two bridging  $\mu_3$ -OR, four  $\mu_2$ -OR, and seven terminal OR units. All Eu atoms are roughly octahedrally six-coordinated. The BVS analysis<sup>29</sup> indicates that four of the Eu atoms are trivalent and one (Eu1) in the basal plane is divalent. The presence of  $\text{Eu}^{2+}$  is more pronounced in one (Eu1–Eu5) of

(25) Kritikos, M.; Moustiakimov, M.; Wijk, M.; Westin, G. *J. Chem. Soc., Dalton Trans.* **2001**, 13, 1927.

(26) Westin, G.; Norrestam, R.; Nygren, M.; Wijk, M. *J. Solid State Chem.* **1998**, 135, 149.

(27) Yatsimirskii, K. B.; Davidenko, N. K. *Coord. Chem. Rev.* **1979**, 27, 223.

(28) Westin, G.; Wijk, M.; Moustiakimov, M.; Kritikos, M. *J. Sol-Gel Sci. Technol.* **1998**, 13, 125.

(29) Brown, I. D.; Altermatt, D. *Acta Crystallogr.* **1985**, B41, 244.

**Table 2.** Selected Bond Lengths<sup>a</sup> for One of the Two [Eu<sub>5</sub>O(OPr<sup>i</sup>)<sub>12</sub>(HOPr<sup>i</sup>)]\*<sup>+</sup>[HOPr<sup>i</sup>] Molecules in **1**

terminal Eu–O		$\mu_2$ Eu–O	
Eu(1)–O(12)	2.558(15)	Eu(1)–O(3)	2.526(13)
Eu(2)–O(10)	2.113(13)	Eu(1)–O(7)	2.458(12)
Eu(3)–O(13)	2.111(16)	Eu(2)–O(3)	2.305(13)
Eu(4)–O(1)	2.094(11)	Eu(2)–O(9)	2.309(11)
Eu(5)–O(11)	2.106(12)	Eu(3)–O(4)	2.262(12)
		Eu(3)–O(7)	2.234(13)
$\mu_3$ Eu–O		Eu(4)–O(4)	
Eu(1)–O(2)	2.603(15)	Eu(4)–O(9)	2.306(14)
Eu(1)–O(5)	2.616(11)		
Eu(2)–O(5)	2.471(10)	$\mu_5$ Eu–O	
Eu(2)–O(8)	2.514(15)	Eu(1)–O(29)	2.612(11)
Eu(3)–O(2)	2.452(11)	Eu(2)–O(29)	2.389(11)
Eu(3)–O(6)	2.532(12)	Eu(3)–O(29)	2.381(10)
Eu(4)–O(6)	2.446(14)	Eu(4)–O(29)	2.419(10)
Eu(4)–O(8)	2.483(11)	Eu(5)–O(29)	2.378(10)
Eu(5)–O(2)	2.321(14)		
Eu(5)–O(5)	2.365(12)	Eu(1)–O(14)	2.956(13)
Eu(5)–O(6)	2.423(11)		
Eu(5)–O(8)	2.329(14)		

<sup>a</sup> Bond lengths are given in angstroms.

the molecules than in the other (Eu6–Eu10). To reach charge neutrality, one of the 2-propoxo groups should be protonated. The distances of approximately 2.6 Å between some of the O atoms of the host Eu<sub>5</sub>O(OPr<sup>i</sup>)<sub>12</sub>(HOR) and the guest HOR molecule suggest the presence of H-bonding. The bent Eu–O–C angle of 155.4(16)° also indicate that the terminal 2-propoxo group on the divalent Eu1 atom is protonated. The OH stretch band in the IR spectra corroborates the presence of hydrogen bonds.

It is interesting to compare the structure of the above-described (Eu<sup>3+</sup>)<sub>4</sub>(Eu<sup>2+</sup>)O unit with the related unit in the (Eu<sup>3+</sup>)<sub>5</sub>O(OPr<sup>i</sup>)<sub>13</sub> (**2**) molecule.<sup>9</sup> There is no substantial difference in geometry between the metal cores of the two molecules, although in **1** it is obviously a bit more distorted from ideal pyramid shape. The major difference, not surprisingly, is in the coordination of the Eu<sup>2+</sup> ion, as can be seen in Figure 5. The average Eu<sup>2+</sup>–O distance in **1** is about 2.5 Å, and Eu<sup>3+</sup>–O in **2** is about 2.3 Å, which is comparable with other similar Eu<sup>2+</sup> and Eu<sup>3+</sup> compounds.<sup>11</sup> The most striking contrast in metal–oxygen distances appears when the oxygen belongs to a terminal OPr<sup>i</sup> group; in this case it is 2.56 Å for **1** and 2.13 Å for **2**.

#### 4. Conclusions

A novel mixed-valence europium 2-propoxide, [Eu<sub>4</sub>EuO(OPr<sup>i</sup>)<sub>12</sub>(HOPr<sup>i</sup>)]\*<sup>+</sup>HOPr<sup>i</sup> (**1**), has been prepared by different synthetic routes: by metathesis combined with stoichiometric hydrolysis, and by oxidation with O<sub>2</sub> and reduction with the metal or [Eu<sub>4</sub>(OPr<sup>i</sup>)<sub>10</sub>(HOPr<sup>i</sup>)<sub>3</sub>]\*<sup>+</sup>2HOPr<sup>i</sup>; the former route is the one most easy to control. This means that **1**, having an average oxidation state of +2.8, can be reached both by reduction of Eu<sub>5</sub>O(OPr<sup>i</sup>)<sub>13</sub> (+3) and by oxidation of [Eu<sub>4</sub>-

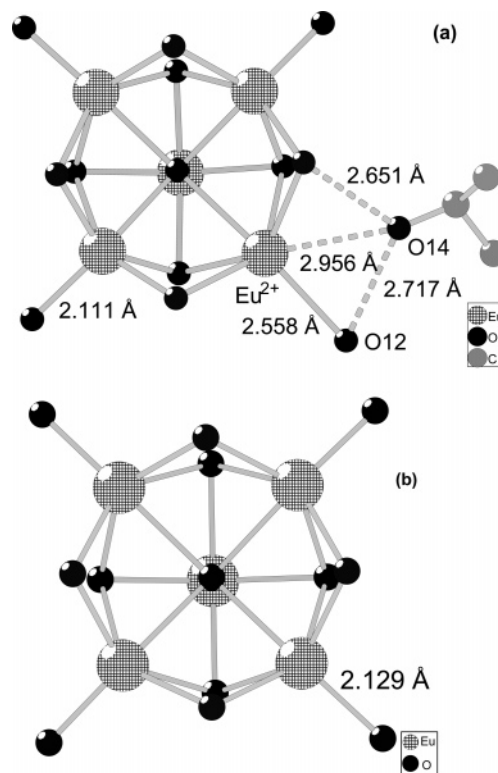


**Figure 5.** Comparison of (Eu<sup>3+</sup>)<sub>4</sub>(Eu<sup>2+</sup>)O(OPr<sup>i</sup>)<sub>12</sub>(HOPr<sup>i</sup>)\*HOPr<sup>i</sup> (a) with (Eu<sup>3+</sup>)<sub>5</sub>O(OPr<sup>i</sup>)<sub>13</sub> (b).

(OPr<sup>i</sup>)<sub>10</sub>(HOPr<sup>i</sup>)<sub>3</sub>]\*<sup>+</sup>2HOPr<sup>i</sup> (+2.5), which places **1** in an interesting redox series of europium 2-propoxides.

IR and UV–vis spectroscopic studies of **1** showed that the molecular structure remained nearly intact on dissolution in hexane or toluene/HOPr<sup>i</sup> solvents. The square pyramidal molecular structure, determined by single-crystal X-ray techniques, is very similar to that of the previously reported Eu<sub>5</sub>O(OPr<sup>i</sup>)<sub>13</sub> but with one of the basal-plane Eu<sup>3+</sup>–OPr<sup>i</sup> links replaced by Eu<sup>2+</sup>–HOPr<sup>i</sup>. This is first example of an Ln<sub>5</sub>O(OPr<sup>i</sup>)<sub>13</sub> molecule with low-valent ion substitution in the basal plane of the Ln<sub>5</sub> square pyramid. This could present valuable information when attempting compositional modification of oxoalkoxides to be used as precursors in the sol–gel preparation of advanced ceramic thin films and nanomaterials or as organic catalysts with tuned properties.

**Acknowledgment.** The Swedish Science Council (VR) is thanked for financing this work. We also thank Dr. K. Jansson, Inorganic Chemistry, Stockholm University, for performing the DSC measurements.

**Supporting Information Available:** X-ray crystallographic file for **1** (CIF). This information is available free of charge via the Internet at <http://pubs.acs.org>.

IC048575A